

On the primary beam deceleration in the pulsar wind

L. I. Arzamasskiy^{1*}, V. S. Beskin^{1,2*}, V. V. Prokofev¹

¹*Moscow Institute of Physics and Technology, Dolgoprudny, Institutskiy per., 9, Moscow region, 141700, Russia*

²*P.N.Lebedev Physical Institute, Leninsky prosp., 53, Moscow, 119991, Russia*

Accepted. Received; in original form

ABSTRACT

We investigate the motion of the primary beam outside the light cylinder in the pulsar wind. Inside the light cylinder both primary and secondary plasma move along dipole magnetic field lines where their energies can be arbitrary. But at larger distances the theory predicts quasi-radial motion with the velocity exactly corresponding to the drift velocity which cannot be the same for primary and secondary plasma. Hence, the deceleration of the primary beam is to take place simultaneously resulting in the acceleration of the secondary plasma. We investigate this process in the three-fluid MHD approximation and demonstrate that for most pulsars the energy of the beam remains practically unchanged. Only for young radio pulsars (Crab, Vela) essential deceleration up to the energy of the secondary plasma takes place outside the fast magnetosonic surface $r_F \sim (10\text{--}100)R_L$, the energy of secondary plasma itself increasing insufficiently.

Key words: Neutron stars – radio pulsars

1 INTRODUCTION

According to the common point of view, the activity of radio pulsars is connected with the electron-positron plasma generated near magnetic poles (Manchester & Taylor 1977; Smith 1977). Numerous works devoted to this subject (Sturrock 1971; Ruderman & Sutherland 1975; Arons 1981; Daugherty & Harding 1982; Gurevich & Istomin 1985; Istomin & Sobyanin 2007; Medin & Lai 2007; Timokhin & Arons 2013) demonstrate that the outflowing plasma consists of the primary beam with the Lorentz-factor $\gamma^b \sim 10^7$ and the number density $n^b \approx n_{GJ}$, where $n_{GJ} = \Omega B / 2\pi c e$ is the Goldreich-Julian number density, and the secondary electron-positron plasma with $n^\pm \sim (10^3\text{--}10^5)n_{GJ}$, and $\gamma^\pm \sim 10^2$.

It is clear that inside the light cylinder $r < R_L = c/\Omega$ both the primary beam and the secondary plasma move along the dipole magnetic field lines where their energies can be arbitrary. On the other hand, at large enough distances from a neutron star $r \gg R_L$ both the analytical theory (Michel 1994; Beskin et al. 1998) and numerical simulations (Contopoulos et al. 1999; Spitkovsky 2006; Tchekhovskoy et al. 2013; Philippov & Spitkovsky 2014) predict the quasi-radial outflow of the relativistic electron-positron plasma along the poloidal magnetic field with the radial velocity exactly corresponding to the drift motion

$$\mathbf{U}_{\text{dr}} = c \frac{\mathbf{E} \times \mathbf{B}}{B^2}. \quad (1)$$

Clearly, this drift velocity cannot describe simultaneously the motion of the beam and the secondary plasma which have sufficiently different energies.

Thus, the question arises about the energy evolution of these two components as they escape the pulsar magnetosphere and propagate outwards forming the pulsar wind. We show that efficient deceleration of primary beam can be realized for young energetic radio pulsars (Crab, Vela) only. In this case the deceleration up to the energy of the secondary plasma takes place outside the fast magnetosonic surface $r_F \sim (10\text{--}100)R_L$, the energy of secondary plasma itself increases insufficiently. For ordinary pulsars with period $P \sim 1$ s, the energy of the primary beam (due to escaping to the region with rather small electric and magnetic fields) remains practically unchanged.

The paper is organized as follows. We start with the description of basic equations of three-fluid MHD in Sect. 2. In Sect. 3 we describe the general properties of these equations. The beam damping is discussed in Sect. 4. Finally, in Sect. 5 the main results of our consideration are formulated.

2 BASIC EQUATIONS

In this section we derive the basic three-fluid MHD equations. Throughout the paper we use the spherical coordinate system (r, θ, φ) with unit vectors $(\mathbf{e}_r, \mathbf{e}_\theta, \mathbf{e}_\varphi)$. All quantities having the superscript 'b' correspond to the primary beam, and the quantities with superscript '±' refer to the

* E-mail: lev.arzamasskiy@phystech.edu, beskin@lpi.ru

secondary plasma particles (electrons or positrons). Finally, electron charge equals $-e$.

To describe the deceleration of the primary beam (and possible acceleration of the secondary plasma) we start from the well-known Michel (1994) monopole force-free solution

$$B_r = B_L \frac{R_L^2}{r^2}, \quad (2)$$

$$E_\theta = B_\varphi = -B_L \frac{R_L}{r} \sin \theta, \quad (3)$$

corresponding to the zero particle mass m_e . Within this approximation, the particles move radially with the velocity $v = c$, so that the current density $j_r = c\rho_e$ and the charge density

$$\rho_e = -\frac{\Omega B_r}{2\pi c} \cos \theta \quad (4)$$

just corresponding to Goldreich-Julian charge density

$$\rho_{\text{GJ}} = -\frac{\Omega \mathbf{B}}{2\pi c}. \quad (5)$$

One can easily check that the fields (2)–(3) with the charge density ρ_e (4) and the current density $j_r = c\rho_e$ are the exact solutions of the time-independent Maxwell equations

$$\nabla \cdot \mathbf{E} = 4\pi\rho_e, \quad \nabla \times \mathbf{E} = 0, \quad (6)$$

$$\nabla \cdot \mathbf{B} = 0, \quad \nabla \times \mathbf{B} = \frac{4\pi}{c} \mathbf{j}. \quad (7)$$

For this reason one can model the outflow with the massless particles moving radially with the velocity $\mathbf{v} = c\mathbf{e}_r$ and having the following number density

$$n^\pm = \lambda \frac{\Omega B_L R_L^2}{2\pi c e r^2}, \quad (8)$$

$$n^b = \frac{\Omega B_L R_L^2}{2\pi c e r^2} \cos \theta. \quad (9)$$

Here $\lambda = en_e/|\rho_{\text{GJ}}| \gg 1$ is the so-called multiplication parameter which equals 10^3 – 10^5 for most radio pulsars. In what follows we consider for simplicity the case of $\lambda = \text{const}$. Such a choice corresponds to the equality of the secondary electron and positron number densities.

As one can see, the only difference with our previous works (Beskin & Rafikov 2000; Beskin et al. 2004) is that we consider here not two-component (i.e., secondary electron-positron plasma) but three-component outflow containing also the primary beam having Goldreich-Julian number density $n^b = |\rho_{\text{GJ}}|/e$ and Lorentz-factor $\gamma^b \sim 10^7 \gg \gamma^\pm$. As is shown in Appendix A, this value is in agreement with the radiation reaction force acting on the beam particle as it moves along dipole magnetic field line inside the light cylinder. On the other hand, as is shown in Appendix B, two-stream instability is not effective, and, hence, three-fluid hydrodynamical approximation under consideration is good enough to describe the evolution of the primary beam.

Then, following the papers mentioned above we can include into consideration the finite particle mass as a small disturbance of the force-free solution. One can do it because for magnetically dominated outflow $\sigma \gg 1$, the outflow remains actually radial (Tomimatsu 1994; Beskin et al. 1998). Here

$$\sigma = \frac{\Omega e B_L R_L^2}{4\lambda m c^3} \quad (10)$$

is the Michel magnetization parameter. For ordinary pulsars

($P \sim 1$ s, $B_0 \sim 10^{12}$ G), one has $\sigma \sim 10^3 - 10^4$, and only for the fast ones ($P \sim 0.1 - 0.01$ s, $B_0 \sim 10^{13}$ G), $\sigma \sim 10^5 - 10^6$.

As a result, to find the structure of the flow we have to analyze Maxwell equations (6)–(7) and the equation of motion for all three components:

$$(\mathbf{v}^\pm, \nabla) \mathbf{p}^\pm = \pm e \left(\mathbf{E} + \frac{\mathbf{v}^\pm}{c} \times \mathbf{B} \right), \quad (11)$$

$$(\mathbf{v}^b, \nabla) \mathbf{p}^b = -e \left(\mathbf{E} + \frac{\mathbf{v}^b}{c} \times \mathbf{B} \right). \quad (12)$$

It is convenient to introduce electric potential $\Phi_e(r, \theta)$ and the magnetic flux function $\Psi(r, \theta)$, so that

$$\mathbf{E} = -\nabla \Phi_e(r, \theta), \quad (13)$$

$$\mathbf{B}_p = \frac{\nabla \Psi \times \mathbf{e}_\varphi}{2\pi r \sin \theta}. \quad (14)$$

Then, one can seek the solution in the form

$$n^\pm = \frac{\Omega B_L R_L^2}{2\pi c e r^2} [\lambda + \eta^\pm(r, \theta)], \quad (15)$$

$$n^b = \frac{\Omega B_L R_L^2}{2\pi c e r^2} [\cos \theta + \eta^b(r, \theta)], \quad (16)$$

$$\Phi_e(r, \theta) = \frac{\Omega R_L^2 B_L}{c} [-\cos \theta + \delta(r, \theta)], \quad (17)$$

$$\Psi(r, \theta) = 2\pi B_L R_L^2 [1 - \cos \theta + \varepsilon f(r, \theta)], \quad (18)$$

$$v_r^{\pm, b} = c [1 - \xi_r^{\pm, b}(r, \theta)], \quad (19)$$

$$v_{\theta, \varphi}^{\pm, b} = c \xi_{\theta, \varphi}^{\pm, b}(r, \theta), \quad (20)$$

with the small disturbances η , δ , εf and ξ corresponding to the small perturbations caused by the finite particle mass. Accordingly, using (13) and (14), one can write down

$$B_r = B_L \frac{R_L^2}{r^2} \left(1 + \frac{\varepsilon}{\sin \theta} \frac{\partial f}{\partial \theta} \right), \quad (21)$$

$$B_\theta = -\varepsilon B_L \frac{R_L^2}{r \sin \theta} \frac{\partial f}{\partial r}, \quad (22)$$

$$B_\varphi = B_L \frac{\Omega R_L R_L}{c r} [-\sin \theta - \zeta(r, \theta)], \quad (23)$$

$$E_r = -B_L \frac{\Omega R_L^2}{c} \frac{\partial \delta}{\partial r}, \quad (24)$$

$$E_\theta = B_L \frac{\Omega R_L^2}{c r} \left(-\sin \theta - \frac{\partial \delta}{\partial \theta} \right). \quad (25)$$

Here all deflecting functions are supposed to be $\ll 1$. For $v_r = c$, $v_\theta = 0$, and $v_\varphi = 0$ for all types of particle, we return to the force-free Michel solution.

Now, substituting Eqns. (15)–(25) into Maxwell equations (6)–(7), we obtain to the first-order approximation the following system of linear equations:

$$2(\Delta\eta + \eta^b) + \frac{\partial}{\partial r} \left(r^2 \frac{\partial \delta}{\partial r} \right) + \frac{1}{\sin \theta} \frac{\partial}{\partial \theta} \left(\sin \theta \frac{\partial \delta}{\partial \theta} \right) = 0, \quad (26)$$

$$\frac{1}{2 \sin \theta} \frac{\partial}{\partial \theta} (\zeta \sin \theta) = \lambda \Delta \xi_r - \xi_r^b \cos \theta - \Delta \eta - \eta^b, \quad (27)$$

$$\frac{\partial \zeta}{\partial r} = \frac{2}{r} (\lambda \Delta \xi_\theta - \xi_\theta^b \cos \theta), \quad (28)$$

$$\begin{aligned} \frac{\varepsilon}{\sin \theta} \frac{\partial^2 f}{\partial r^2} + \frac{\varepsilon}{r^2} \frac{\partial}{\partial \theta} \left(\frac{1}{\sin \theta} \frac{\partial f}{\partial \theta} \right) = \\ = 2 \frac{\Omega}{rc} (\cos \theta \xi_\varphi^b - \lambda \Delta \xi_\varphi). \end{aligned} \quad (29)$$

Accordingly, equations of motion (11) and (12) now looks

like

$$\begin{aligned} \frac{\partial}{\partial r} (\xi_\theta^\pm \gamma^\pm) + \frac{\xi_\theta^\pm \gamma^\pm}{r} &= \\ &= \pm 4\lambda\sigma \left(-\frac{1}{r} \frac{\partial \delta}{\partial \theta} + \frac{\zeta}{r} - \frac{\sin \theta}{r} \xi_r^\pm + \frac{c}{\Omega r^2} \xi_\varphi^\pm \right), \end{aligned} \quad (30)$$

$$\begin{aligned} \frac{\partial}{\partial r} (\xi_\theta^b \gamma^b) + \frac{\xi_\theta^b \gamma^b}{r} &= \\ &= -4\lambda\sigma \left(-\frac{1}{r} \frac{\partial \delta}{\partial \theta} + \frac{\zeta}{r} - \frac{\sin \theta}{r} \xi_r^b + \frac{c}{\Omega r^2} \xi_\varphi^b \right), \end{aligned} \quad (31)$$

$$\frac{\partial}{\partial r} (\gamma^\pm) = \pm 4\lambda\sigma \left(-\frac{\partial \delta}{\partial r} - \frac{\sin \theta}{r} \xi_\theta^\pm \right), \quad (32)$$

$$\frac{\partial}{\partial r} (\gamma^b) = -4\lambda\sigma \left(-\frac{\partial \delta}{\partial r} - \frac{\sin \theta}{r} \xi_\theta^b \right), \quad (33)$$

$$\begin{aligned} \frac{\partial}{\partial r} (\xi_\varphi^\pm \gamma^\pm) + \frac{\xi_\varphi^\pm \gamma^\pm}{r} &= \\ &= \mp 4\lambda\sigma \left(\varepsilon \frac{c}{\Omega r \sin \theta} \frac{\partial f}{\partial r} + \frac{c}{\Omega r^2} \xi_\theta^\pm \right), \end{aligned} \quad (34)$$

$$\begin{aligned} \frac{\partial}{\partial r} (\xi_\varphi^b \gamma^b) + \frac{\xi_\varphi^b \gamma^b}{r} &= \\ &= 4\lambda\sigma \left(\varepsilon \frac{c}{\Omega r \sin \theta} \frac{\partial f}{\partial r} + \frac{c}{\Omega r^2} \xi_\theta^b \right). \end{aligned} \quad (35)$$

Here $\Delta A = A^+ - A^-$, so these terms vanish in one fluid MHD description.

Formally, the system of equations (26)–(35) requires fifteen boundary conditions. We consider for simplicity the case $\Omega R/c \ll 1$ when the star radius R is much smaller than the light cylinder. As a result, one can write down the first nine boundary conditions as

$$\xi_\theta^\pm(R_L, \theta) = 0, \quad (36)$$

$$\xi_\theta^b(R_L, \theta) = 0, \quad (37)$$

$$\xi_\varphi^b(R_L, \theta) = 0, \quad (38)$$

$$\xi_\varphi^\pm(R_L, \theta) = 0, \quad (39)$$

$$\gamma^\pm(R_L, \theta) = \gamma_{\text{in}}, \quad (40)$$

$$\gamma^b(R_L, \theta) = \gamma_{\text{in}}^b, \quad (41)$$

where γ_{in} and γ_{in}^b are the initial Lorentz-factors of secondary plasma and beam particles correspondingly.

Finally, as a boundary conditions one can put

$$\delta(R_L, \theta) = 0, \quad (42)$$

$$\varepsilon f(R_L, \theta) = 0, \quad (43)$$

$$\eta^+(R_L, \theta) - \eta^-(R_L, \theta) = 0, \quad (44)$$

$$\eta^b(R_L, \theta) = 0, \quad (45)$$

resulting from the relation $\mathbf{E}_L + (\Omega R_L/c) \mathbf{e}_\varphi \times \mathbf{B}_L = 0$ which implies a rigid rotation and a perfect conductivity of the surface of a star. It is necessary to stress that all the expressions are valid only for a quasi-monopole outflow which exists only outside the light cylinder.

3 GENERAL PROPERTIES

It is clear that in general case the analytical solution of Eqns. (26)–(35) cannot be found. On the other hand, this system of equation contains some integrals of motion which allow us to obtain the necessary information about the energy of the

outflowing particles. In particular, as was demonstrate by Beskin & Rafikov (2000), in the two-fluid approximation this approach reproduces well-known one-fluid MHD results for the position of the fast magnetosonic surface for $\gamma_{\text{in}} \ll \sigma^{1/3}$

$$r_F = \sigma^{1/3} \sin^{-1/3} \theta R_L \quad (46)$$

and the Lorentz-factor at this surface $\gamma_F = \gamma^\pm(r_F)$

$$\gamma_F = \sigma^{1/3} \sin^{2/3} \theta. \quad (47)$$

Below we show that it is true for $\gamma_{\text{in}} \gg \sigma^{1/3}$ as well.

First of all, excluding ξ_θ^\pm and ξ_θ^b from Eqn. (28) and using (32) and (33) we obtain the following equation

$$\begin{aligned} \frac{\partial \zeta}{\partial r} &= \frac{2}{\tan \theta} \frac{\partial \delta}{\partial r} - \\ &- \frac{1}{2\sigma \sin \theta} \left(\frac{\partial \gamma^+}{\partial r} + \frac{\partial \gamma^-}{\partial r} \right) - \frac{1}{2\sigma \lambda \tan \theta} \frac{\partial \gamma^b}{\partial r}. \end{aligned} \quad (48)$$

It gives

$$\begin{aligned} \zeta - \frac{2}{\tan \theta} \delta + \frac{\lambda(\gamma^+ + \gamma^-) + (\gamma^b - \gamma_{\text{in}}^b) \cos \theta}{2\lambda\sigma \sin \theta} &= \\ &= \frac{1}{\sigma \sin \theta} \gamma_{\text{in}} + \frac{l(\theta)}{\sin \theta}, \end{aligned} \quad (49)$$

where $\zeta(0, \theta) = l(\theta)/\sin \theta$ and $l(\theta)$ describes the disturbance of the electric current. Expression (49) corresponds to the conservation of the total energy flux along a magnetic field line. On the other hand, combining Eqns. (32)–(35), one can obtain the expressions corresponding to conversation of the z -component of the angular momentum for all types of particles

$$\delta = \varepsilon f \mp \frac{1}{4\lambda\sigma} \gamma^\pm \left(1 - \frac{\Omega r \sin \theta}{c} \xi_\varphi^\pm \right) \pm \frac{1}{4\lambda\sigma} \gamma_{\text{in}}, \quad (50)$$

$$\delta = \varepsilon f + \frac{1}{4\lambda\sigma} \gamma^b \left(1 - \frac{\Omega r \sin \theta}{c} \xi_\varphi^b \right) - \frac{1}{4\lambda\sigma} \gamma_{\text{in}}^b. \quad (51)$$

Now, neglecting the difference between γ^+ and γ^- so that $\xi^+ = \xi^-$ and $\gamma^+ = \gamma^- = \gamma$ (which can be done in case of $\sigma \gg 1$ and $\lambda \gg 1$), we obtain

$$\delta = \varepsilon f, \quad (52)$$

and, hence,

$$\gamma \left(1 - \frac{\Omega r \sin \theta}{c} \xi_\varphi \right) = \gamma_{\text{in}}. \quad (53)$$

Accordingly, from (51) we have

$$\gamma^b \left(1 - \frac{\Omega r \sin \theta}{c} \xi_\varphi^b \right) = \gamma_{\text{in}}^b. \quad (54)$$

On the other hand, Eqn. (33) for $\lambda\sigma \gg 1$ gives

$$-\frac{1}{r} \frac{\partial \delta}{\partial \theta} + \frac{\zeta}{r} - \frac{\sin \theta}{r} \xi_r + \frac{c}{\Omega r^2} \xi_\varphi = 0. \quad (55)$$

Further, using the definitions (19)–(20) to describe γ in terms of ξ_r and ξ_θ , and neglecting ξ_θ , one can write down

$$\gamma^2 = \frac{1}{2\xi_r - \xi_\theta^2}. \quad (56)$$

As a result, combining relations (53), (55), (56), and (56), one can finally find the following algebraic equation on the hydrodynamical Lorentz-factor of the secondary plasma γ

$$2\gamma^3 - 2\sigma \left[K + \frac{1}{2x^2} + \frac{\gamma_{\text{in}}}{\sigma} \right] \gamma^2 + \sigma \sin^2 \theta + \sigma \frac{c^2 \gamma_{\text{in}}^2}{\Omega^2 r^2} = 0, \quad (57)$$

where $x = r/R_L$ and

$$K(r, \theta) = 2 \cos \theta \delta - \sin \theta \frac{\partial \delta}{\partial \theta} - \frac{\gamma^b - \gamma_{\text{in}}^b}{2\sigma\lambda} \cos \theta + \frac{l(\theta)}{\sin \theta}. \quad (58)$$

Equations (57)–(58) generalize the appropriate ones obtained by Beskin & Rafikov (2000) for two-component plasma and for $\gamma_{\text{in}} \ll \sigma^{1/3}$. As was already stressed, these equations allow us to find the position of fast magnetosonic surface corresponding to the intersection of two roots of algebraic equation (57). Indeed, determining the derivative $r\partial\gamma/\partial r$, one can obtain

$$r \frac{\partial \gamma}{\partial r} = \gamma \sigma \frac{r \partial K / \partial r - x^{-2} [1 - (\gamma_{\text{in}}/\gamma)^2]}{3\gamma - 2\gamma_{\text{in}} - \sigma(2K + x^{-2})}. \quad (59)$$

As the fast magnetosonic surface is the X -point, both the numerator and denominator are both equal to zero there. As a result, evaluating $r\partial K/\partial r$ as K , we obtain the following well-known asymptotic solutions (Bogovalov 2001):

(i) Fast rotator ($\gamma_{\text{in}} < \sigma^{1/3}$). In this case we may neglect the terms containing γ_{in} . It gives for $\delta_{\text{F}} = \delta(r_{\text{F}})$, etc.

$$\delta_{\text{F}} \approx \sigma^{-2/3}, \quad (60)$$

$$r_{\text{F}} \approx \sigma^{1/3} \sin^{-1/3} \theta R_L, \quad (61)$$

$$\gamma_{\text{F}} = \sigma^{1/3} \sin^{2/3} \theta, \quad (62)$$

the last expression being exact. As we see, for fast rotator the acceleration of the secondary plasma from $\gamma = \gamma_{\text{in}}$ to $\gamma = \sigma^{1/3}$ takes place up to the fast magnetosonic surface.

(ii) Slow rotator ($\gamma_{\text{in}} > \sigma^{1/3}$). In this case we obtain

$$\delta_{\text{F}} \approx \gamma_{\text{in}} \sigma^{-1}, \quad (63)$$

$$r_{\text{F}} \approx \sigma^{1/2} \gamma_{\text{in}}^{-1/2} R_L, \quad (64)$$

$$\gamma_{\text{F}} \approx \gamma_{\text{in}}. \quad (65)$$

For slow rotator there is no particle acceleration within the fast magnetosonic surface which has a spherical shape.

4 BEAM DAMPING AND PLASMA ACCELERATION

4.1 Beam damping

In this section we determine how the energy of the primary beam changes as it outflows from the pulsar magnetosphere. As we consider the secondary plasma in the MHD limit where there is no longitudinal electric field, we may neglect the term $\partial\delta/\partial r$. This leads to the simple determination of ξ_{θ}^b from Eqn. (33):

$$\xi_{\theta}^b \approx \frac{r}{4\lambda\sigma} \frac{\partial \gamma^b}{\partial r}, \quad (66)$$

where we also consider the case $\sin \theta \sim \cos \theta \sim 1$. On the other hand, for $\lambda\sigma \gg 1$ one can set the quantity in brackets in Eqn. (30) equal to zero. After that we can rewrite Eqn. (31) in the following way:

$$\frac{\partial}{\partial r} (r \xi_{\theta}^b \gamma^b) = 4\lambda\sigma \left[\xi_r^b - \xi_r - \frac{r}{R_L} (\xi_{\varphi}^b - \xi_{\varphi}) \right]. \quad (67)$$

Now, using Eqs. (53)–(54), (56) and the definition

$$\xi_r^b = \frac{1}{2(\gamma^b)^2} + \frac{(\xi_{\varphi}^b)^2}{2}, \quad (68)$$

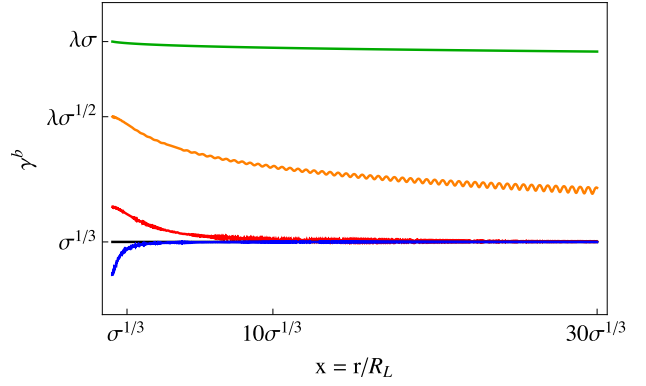


Figure 1. The evolution of the beam Lorentz-factor $\gamma^b(x)$ for different initial energies $m_e c^2 \gamma_{\text{in}}^b$ (see text for more detail).

one can finally obtain the following general equation describing the beam damping:

$$\frac{\partial}{\partial x} \left(x^2 \frac{\partial p}{\partial x} \right) = \Lambda^2 \left(\frac{1}{(\gamma_{\text{in}}^b)^2} \frac{1}{p+1} - \frac{1}{\gamma^2} - \frac{1}{x^2} \frac{p}{p+1} + \frac{\Delta}{x^2} \right). \quad (69)$$

Here we use the following notations

$$p = \frac{(\gamma^b)^2 - (\gamma_{\text{in}}^b)^2}{(\gamma_{\text{in}}^b)^2}, \quad \Lambda = \frac{4\lambda\sigma}{\gamma_{\text{in}}^b}, \quad \Delta = \frac{\gamma^2 - \gamma_{\text{in}}^2}{\gamma^2}. \quad (70)$$

The solutions of equation (69) for different initial energy $m_e c^2 \gamma_{\text{in}}^b$ of a beam (and for $\gamma_{\text{in}} = \gamma = \sigma^{1/3}$) are presented on Figure 1. As we see, for very large initial Lorentz-factor of a beam $\gamma_{\text{in}}^b > \lambda\sigma$ (green line), its energy remains actually constant. The point is that the Larmor radius $r_L = m_e c^2 \gamma^b / e B_L$ for such a large energy of a beam is much larger than the light cylinder radius R_L so the electromagnetic fields cannot disturb the radial motion of the beam. But, as we see, for $\gamma_{\text{in}}^b \approx \lambda\sigma^{1/2}$, when $r_L \approx R_L$ (orange line), the curve has oscillations corresponding to rotation in the comoving reference frame and beam energy slightly damps.

On the other hand, for smaller Lorentz-factors of the beam $\gamma_{\text{in}} < \gamma_{\text{in}}^b < \lambda\sigma^{1/2}$ (red line) the beam energy marginally damps to the energy of secondary plasma. Here again the oscillations correspond to the rotation in the comoving reference frame. For $\gamma_{\text{in}}^b = \gamma = \sigma^{1/3}$ (black line), the energy of the beam remains unchanged. Finally, if the initial energy of the beam is relatively close to the energy of the secondary plasma, the beam either damps or accelerates to the secondary plasma energy. Although the case of $\gamma_{\text{in}}^b < \gamma$ (blue line) is impossible in real pulsars, this solution describes the behaviour of secondary particles: if their initial Lorentz-factor is less than $\sigma_M^{1/3}$, they become accelerated to this energy.

For sufficiently large initial Lorentz-factors of the beam, one can put $p \ll 1$ and neglect the second term in (69). In this case Eqn. (69) becomes linear, and one could solve it using Green's function:

$$p(x) = \Lambda^2 \int_1^x dx' \sin \left(\frac{\Lambda}{x} - \frac{\Lambda}{x'} \right) \left[\frac{1}{\gamma^2(x')} + \frac{\Delta(x')}{x'^2} \right]. \quad (71)$$

After transition to the limit $x \rightarrow \infty$, we obtain the following asymptotic solution:

$$p(x) \simeq - \left(\frac{\Lambda}{\gamma_{\text{out}}^b} \right)^2 [\ln(x/\Lambda) - \Gamma]. \quad (72)$$

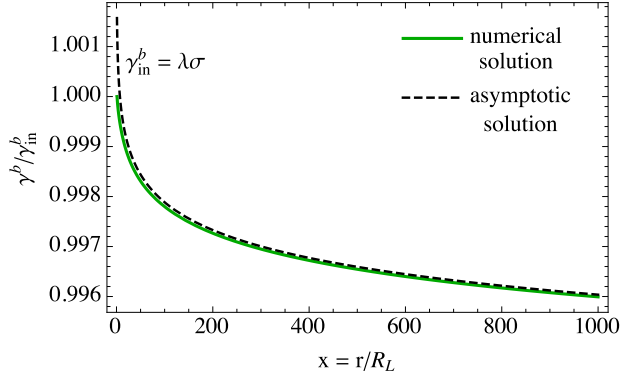


Figure 2. Evolution of the Lorentz-factor of the beam for $\gamma_{\text{in}}^{\text{b}} = \lambda\sigma$. Green solid line represents numerical solution of exact equation (69) and black dashed line describes analytical asymptotic solution (72).

Here

$$\gamma_{\text{out}} = \lim_{x \rightarrow \infty} \gamma(x), \quad (73)$$

and $\Gamma \simeq 1\text{--}10$ is a constant which weakly depends on behavior of $\gamma(x)$ and Λ . For constant γ and $\Lambda \gtrsim 1$, this value is equal to the Euler-Mascheroni constant $\Gamma \approx 0.577$.

Approximating now $\ln(x/\Lambda) - \Gamma \sim 1$, one can finally obtain the following equation describing Lorentz-factor of the primary particles:

$$(\gamma_{\text{out}}^{\text{b}})^2 = (\gamma_{\text{in}}^{\text{b}})^2 - (4\lambda\sigma/\gamma_{\text{out}})^2. \quad (74)$$

Hence, as was already found, large enough disturbance of the energy of the primary beam $\Delta\gamma^{\text{b}} \simeq \gamma_{\text{in}}^{\text{b}}$ is valid only if the condition $\gamma_{\text{in}}^{\text{b}} < \lambda\sigma^{1/2}$ holds. For $\gamma_{\text{in}}^{\text{b}} > \lambda\sigma$ the energy of the beam remains actually unchanged. Figure 2 illustrates the evolution of $\gamma^{\text{b}}(r)$ according to the numerical solution of Eqn. (69) in comparison with analytical solution (72). As we see, they are in a very good agreement. To summarize, the beam energy stabilizes at the following values:

$$\gamma_{\text{out}}^{\text{b}} = \gamma_{\text{in}}^{\text{b}}; \quad \gamma_{\text{in}}^{\text{b}} < \lambda\sigma^{1/2}, \quad (75)$$

$$\gamma_{\text{out}} < \gamma_{\text{out}}^{\text{b}} < \gamma_{\text{in}}^{\text{b}}; \quad \lambda\sigma^{1/2} < \gamma_{\text{in}}^{\text{b}} < \lambda\sigma, \quad (76)$$

$$\gamma_{\text{out}}^{\text{b}} = \gamma_{\text{in}}^{\text{b}}; \quad \gamma_{\text{in}}^{\text{b}} > \lambda\sigma, \quad (77)$$

where γ_{out} is the final Lorentz-factor of the secondary plasma (see below).

Note, that if $\gamma_{\text{in}}^{\text{b}} > \lambda\sigma$, the pulsar total energy losses are less than the beam energy. This case is thus unphysical.

4.2 Secondary plasma acceleration

We are now in position to evaluate the final Lorentz-factor of the secondary plasma γ_{out} . For this we look for the solution of equation (57) in the limit $x \rightarrow \infty$. Neglecting the disturbance of electric current we can approximate $K(r, \theta)$ in Eqn. (58) as

$$K_{\infty} = \delta_{\infty} - \frac{\gamma_{\text{out}}^{\text{b}} - \gamma_{\text{in}}^{\text{b}}}{2\sigma\lambda}. \quad (78)$$

At large distances outside the fast magnetosonic surface we can neglect two last terms in equation (57), which gives us

a simple expression for γ_{out} :

$$\gamma_{\text{out}} = \gamma_{\text{in}} + \sigma \left(\delta_{\infty} - \frac{\gamma_{\text{out}}^{\text{b}} - \gamma_{\text{in}}^{\text{b}}}{2\lambda\sigma} \right). \quad (79)$$

According to Eqns. (60), (63), $\delta_{\infty} \sim \max(\sigma^{-2/3}, \gamma_{\text{in}}\sigma^{-1})$, so we approximate equation (79) as

$$\gamma_{\text{out}} = \max(\sigma^{1/3}, \gamma_{\text{in}}) - \frac{\gamma_{\text{out}}^{\text{b}} - \gamma_{\text{in}}^{\text{b}}}{2\lambda}. \quad (80)$$

In what follows we consider for simplicity the case $\gamma_{\text{in}} \ll \sigma^{1/3}$, but our results could be easily generalized for the opposite case.

Note, that equation (80) sets γ_{out} implicitly since $\gamma_{\text{out}}^{\text{b}}$ depends on γ_{out} :

$$\gamma_{\text{out}}^{\text{b}} - \gamma_{\text{in}}^{\text{b}} \approx \frac{(\gamma_{\text{out}}^{\text{b}})^2 - (\gamma_{\text{in}}^{\text{b}})^2}{2\gamma_{\text{in}}^{\text{b}}} = \frac{\gamma_{\text{in}}^{\text{b}}}{2} p_{\text{out}}(\gamma_{\text{out}}). \quad (81)$$

This approximation is valid only when the beam damping is small, i.e., for large enough $\gamma_{\text{in}}^{\text{b}}$. In this limit, using equation (72), we finally obtain

$$\gamma_{\text{out}} = \sigma^{1/3} + \frac{4\lambda\sigma^2}{\gamma_{\text{in}}^{\text{b}}\gamma_{\text{out}}^2}. \quad (82)$$

For very large $\gamma_{\text{in}}^{\text{b}}$, one can put $\gamma_{\text{out}} = \gamma_{\text{in}} = \sigma^{1/3}$, so both the beam and the secondary plasma do not change their energy. But there is a range of the value $\gamma_{\text{in}}^{\text{b}}$, where the second term in Eqn. (82) is larger than the first one. For such parameters

$$\gamma_{\text{out}} \sim \frac{\lambda^{1/3}\sigma^{2/3}}{(\gamma_{\text{in}}^{\text{b}})^{1/3}}. \quad (83)$$

Finally, for sufficiently small $\gamma_{\text{in}}^{\text{b}}$, one can put $\gamma_{\text{out}}^{\text{b}} = \sigma^{1/3}$. Then, for $\lambda \gg 1$ equation (80) transforms into

$$\gamma_{\text{out}} = \sigma^{1/3} + \frac{\gamma_{\text{in}}^{\text{b}}}{2\lambda}. \quad (84)$$

Thus, for small enough initial energy of the beam, the energy of the secondary particles linearly increases with $\gamma_{\text{in}}^{\text{b}}$.

One can now construct the following approximate expression, which is valid in both limits

$$\gamma_{\text{out}} = \sigma^{1/3} + \left[\left(\frac{\gamma_{\text{in}}^{\text{b}}}{2\lambda} \right)^{-1} + \left(\frac{\lambda^{1/3}\sigma^{2/3}}{(\gamma_{\text{in}}^{\text{b}})^{1/3}} \right)^{-1} \right]^{-1} \quad (85)$$

and determine the maximum gamma factor of the secondary plasma:

$$\gamma_{\text{out}}^{\text{max}} \sim \sigma^{1/2}, \quad \text{for } \gamma_{\text{in}}^{\text{b}} = \lambda\sigma_{\text{M}}^{1/2}. \quad (86)$$

Figure 3 shows obtained asymptotic behavior (85). The exact location of the maximum is $\gamma_{\text{in}}^{\text{b}} = 6^{3/4}\lambda\sigma_{\text{M}}^{1/2}$ and $\gamma_{\text{out}}^{\text{max}} = \sigma_{\text{M}}^{1/3} + 0.25(3/8)^{3/4}\sigma_{\text{M}}^{1/2} \approx \sigma_{\text{M}}^{1/3} + 0.48\sigma_{\text{M}}^{1/2}$. One should also note that the maximum gamma-factor of the secondary plasma is close to the initial one: even for the fastest pulsars,

$$\gamma_{\text{out}}^{\text{max}}/\gamma_{\text{in}} = \sigma^{1/6} \sim 10. \quad (87)$$

All the expressions written above remains the same in case $\gamma_{\text{in}} \gg \sigma^{1/3}$ as well. The only differences is in first terms of r.h.s of Eqns. (82), (84), and (85), which are replaced on

¹ For $\gamma_{\text{in}}^{\text{b}} < \gamma_{\text{in}}$, equation (80) gives $\gamma_{\text{out}} < \gamma_{\text{in}}$, i.e., the secondary plasma loses energy and accelerates the primary particles

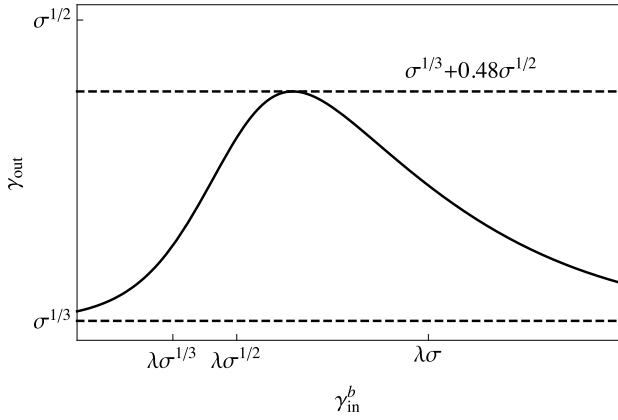


Figure 3. The final Lorentz-factor of the secondary plasma according to Eqn. (85).

γ_{in} instead of $\sigma_M^{1/3}$. This implies that for such pulsars the effect of the pulsar wind acceleration via beam particles is even smaller. For $\gamma_{in} \gg \sigma_M^{1/2}$ this effect vanishes.

5 CONCLUSION

It was demonstrated that the effective deceleration of the primary beam takes place only for relatively small beam energy

$$\gamma_{in}^b < \lambda\sigma^{1/2}. \quad (88)$$

As λ and σ are connected with the relation (Beskin 2010)

$$\sigma\lambda \sim \left(\frac{W_{tot}}{W_A} \right)^{1/2}, \quad (89)$$

where W_{tot} is the total energy losses of a pulsar and $W_A = m_e^2 c^5 / e^2 \approx 10^{17}$ erg/s, one can easily estimate the total number of pulsars having effective damping of the primary beam. Setting $\gamma_{in}^b = 10^7$ and $\lambda = 10^4$, we obtain that among 2003 known radio pulsars with measured P and \dot{P} , only 65 sources have relatively small initial Lorentz-factors $\gamma_{in}^b < \lambda\sigma^{1/2}$.

Thus, one can conclude that effective deceleration of the primary beam takes place only for sufficiently energetic pulsars satisfying the condition $W_{tot} \gtrsim 10^{36}$ erg/s (Crab, Vela). In this case during its motion through the magnetosphere the primary beam decelerates, accelerating simultaneously the secondary particles. But such an additional acceleration is not actually effective enough as the maximum Lorentz-factor of the secondary plasma does not exceed $\sigma^{1/2}$, which is only on the factor $\sigma^{1/6}$ larger than the energy of the secondary plasma near the fast magnetosonic surface. For ordinary pulsars the deceleration of the primary beam can be neglected, so the energy of the primary beam as well as secondary plasma remain constant.

It is very important that the deceleration/acceleration takes place on the scale of the fast magnetosonic surface $r_F \sim \sigma^{1/3} R_L$, i.e., at the distances much larger than the radius of the light cylinder. This implies that even for the fast young radio pulsars the energetic particles of the beam will intersect the magnetospheric current sheet as their velocities exceed the velocity of the secondary plasma which just determines the radial velocity of the current sheet. Indeed,

for fast pulsars the scale $r_F \sim 10^2 R_L$ corresponds to several wave length of the current sheet.

6 ACKNOWLEDGMENTS

We thank A.Spitkovsky, A.Philippov and Y.N. Istomin for their interest and useful discussions. This work was partially supported by Russian Foundation for Basic Research (Grant no. 14-02-00831).

REFERENCES

- Arons J., 1981, ApJ, 248, 1099
Beskin V. S., 2010, MHD Flows in Compact Astrophysical Objects. Springer
Beskin V. S., Kuznetsova I. V., Rafikov R. R., 1998, MNRAS, 299, 341
Beskin V. S., Rafikov R. R., 2000, MNRAS, 313, 433
Beskin V. S., Zakamska N. L., Sol H., 2004, MNRAS, 347, 587
Bogovalov S. V., 2001, A&A, 371, 1155
Contopoulos I., Kazanas D., Fendt C., 1999, ApJ, 511, 351
Daugherty J. K., Harding A. K., 1982, ApJ, 252, 337
Gurevich A. V., Istomin I. N., 1985, Zhurnal Eksperimentalnoi i Teoreticheskoi Fiziki, 89, 3
Istomin Y. N., Sobyenin D. N., 2007, Astronomy Letters, 33, 660
Manchester R. N., Taylor J. H., 1977, Pulsars. W. H. Freeman
Medin Z., Lai D., 2007, MNRAS, 382, 1833
Michel F. C., 1994, ApJ, 431, 397
Philippov A. A., Spitkovsky A., 2014, ApJ, 785, L33
Ruderman M. A., Sutherland P. G., 1975, ApJ, 196, 51
Smith F. G., 1977, Pulsars. Cambridge University Press
Spitkovsky A., 2006, ApJ, 648, L51
Sturrock P. A., 1971, ApJ, 164, 529
Tchekhovskoy A., Spitkovsky A., Li J. G., 2013, MNRAS, 435, L1
Timokhin A. N., Arons J., 2013, MNRAS, 429, 20
Tomimatsu A., 1994, PASJ, 46, 123
Zheleznyakov V. V., 1977, Electromagnetic waves in cosmic plasma. Generation and propagation. Nauka

This paper has been typeset from a $\text{\TeX}/\text{\LaTeX}$ file prepared by the author.

APPENDIX A: RADIATION FORCE DAMPING

Inside the light cylinder the damping of a beam is defined by radiation losses. Outside the acceleration gap the change of the bulk Lorentz-factor of a beam is described by following equation (Zheleznyakov 1977)

$$mc^2 \frac{d\gamma}{dl} = -\frac{2}{3} \frac{e^2}{R_c^2} \gamma^4, \quad (A1)$$

where R_c is the curvature radius of particle trajectory (i.e., the curvature radius of the magnetic field line), and l is a path. For simplify we consider here a dipole structure of magnetic field inside the light cylinder.

Dipole magnetic field lines in polar coordinates are described by the well-known relation $r = r_0 \sin^2 \theta$, where $r_0 \gtrsim R_L$ is a parameter of the line. The appropriate expression in Cartesian coordinates looks like $y =$

$\pm\sqrt{(r_0x^2)^{2/3} - x^2}$. It gives for the curvature radius

$$R_c = r_0 \frac{a^{1/3}(4 - 3a^{2/3})^{3/2}}{(6 - 3a^{2/3})}, \quad (\text{A2})$$

where $a = x/r_0$. Accordingly,

$$dl = \frac{r_0}{3} \sqrt{\frac{4 - 3a^{2/3}}{a^{2/3}(1 - a^{2/3})}} da. \quad (\text{A3})$$

It gives

$$\frac{d\gamma}{\gamma^4} = -\frac{6r_e}{r_0} \int_{R/r_0}^{R_L/r_0} \frac{da}{a} \frac{(2 - a^{2/3})^2}{(4 - 3a^{2/3})^{5/2}(1 - a^{2/3})^{1/2}}. \quad (\text{A4})$$

Here $r_e = e^2/m_e c^2$ is the classical electron radius, and R is the stellar radius. This equation can be easily solved analytically, and we obtain

$$\frac{1}{\gamma_0^3} - \frac{1}{\gamma_{\text{in}}^3} = 24 \frac{r_e}{R_L} \left[2 \left(\ln \frac{R_L}{R} + 1 \right) + F(r_0, R) \right], \quad (\text{A5})$$

where $F(r_0, R) \approx 1$ and, hence, may be neglected. As the initial Lorentz-factor of the primary beam after acceleration inside thin gap is estimated as 10^8 – 10^9 (Beskin 2010), one can neglect the second term in the l.h.s. of Eqn. (A5), and we finally obtain

$$\gamma_0 \sim 0.1 \left(\frac{R_L}{r_e} \right)^{1/3} \sim 10^7. \quad (\text{A6})$$

APPENDIX B: BEAM INSTABILITY

In this section we consider the effects leading to the beam instability and estimate the distance where the beam deceleration by the wave-particle interaction takes place. For simplicity, we use the following expression for plasma dielectric permittivity

$$\varepsilon(\omega, \mathbf{k}) = 1 - \frac{(\omega_p)^2}{\gamma^3(\omega - \mathbf{k}\mathbf{v}_p)^2} - \frac{(\omega_b)^2}{(\gamma^b)^3(\omega - \mathbf{k}\mathbf{v}_b)^2}, \quad (\text{B1})$$

where \mathbf{v}_p and \mathbf{v}_b are the velocities of the secondary plasma and the primary beam respectively, and ω_p and ω_b are corresponding plasma frequencies:

$$\omega_{p,b}^2 = \frac{4\pi e^2 n_{p,b}}{m_e}. \quad (\text{B2})$$

For $\mathbf{k} \parallel \mathbf{v}_b \parallel \mathbf{v}_p$, the spectrum of plasma oscillations (i.e., Langmuir waves) corresponds to the condition $\varepsilon(\omega, \mathbf{k}) = 0$. Considering now the solution as

$$\omega = \mathbf{k}\mathbf{v}_b + \delta\omega, \quad (\text{B3})$$

where $\delta\omega \ll \mathbf{k}\mathbf{v}_b$, one can obtain for the maximum growth increment

$$\delta\omega_{\text{max}} = \kappa \frac{(\omega_p)^{1/3}(\omega_b)^{2/3}}{\gamma^{1/2}\gamma^b} \quad (\text{B4})$$

with $\kappa \approx 1$.

Before becoming unstable, the beam travels the distance

$$d_{\text{stab}} = \frac{c}{\delta\omega_{\text{max}}} \approx \frac{c}{\omega_{\text{GJ}}} \frac{\gamma^{1/2}\gamma^b}{\lambda^{1/6}}, \quad (\text{B5})$$

where $\omega_{\text{GJ}}^2 = 4\pi n_{\text{GJ}} e^2 / m_e = 2\Omega\omega_B$. It gives

$$\begin{aligned} \frac{d_{\text{stab}}}{R_L} &= \left(\frac{\Omega}{\omega_B} \right)^{1/2} \frac{\gamma^{1/2}\gamma^b}{\lambda^{1/6}} = \\ &= 1500 B_6^{-1/2} P_s^{-1/2} \gamma_7^b \gamma_2^{-1/2} \lambda_6^{-1/6} \gg 1. \end{aligned} \quad (\text{B6})$$

Here we assume the value of the magnetic field near the light cylinder to be of order 10^6 G which is natural for fast radio pulsars. Thus, one can conclude that one can neglect the two-fluid instability within distances which were considered in this paper.

One can find even more precise expressions considering the values ω_b , $\omega_p \propto r^{-1}$ as depending on the radius r , as it takes place in Michel solution (2)-(3). The destruction distance could then be found from

$$\int_{R_L}^{R_L + d_{\text{stab}}} \frac{\omega_p^{2/3}(r)\omega_b^{1/3}(r) dr}{\gamma(\gamma^b)^{1/2} c} = 1. \quad (\text{B7})$$

Assuming now that $\gamma_{p,b}$ do not depend on r , we obtain

$$\begin{aligned} \log \left(\frac{R_L + d_{\text{stab}}}{R_L} \right) &= \frac{c\gamma^b}{R_L \omega_p^{2/3}(R_L) \omega_b^{1/3}(R_L)} = \\ &= 1500 B_8^{-1/2} P_s^{-1/2} \gamma_7^b \gamma_2^{-1/2} \lambda_6^{-1/6} \gg 1. \end{aligned} \quad (\text{B8})$$

Thus, in reality not only the condition $d_{\text{stab}}/R_L \gg 1$, but much more strong one

$$\log(d_{\text{stab}}/R_L) \gg 1 \quad (\text{B9})$$

is valid.

This paper has been typeset from a $\text{\TeX}/\text{\LaTeX}$ file prepared by the author.